Highlights of Spanish Astrophysics VII, Proceedings of the X Scientific Meeting of the Spanish Astronomical Society held on July 9 - 13, 2012, in Valencia, Spain. J. C. Guirado, L. M. Lara, V. Quilis, and J. Gorgas (eds.)

Mid-infrared emission of AGN using RedCan

O. González-Martín[1,2,3], J.M. Rodríguez-Espinosa[1,2], T. Díaz-Santos[4], C.Packham[5], A. Alonso-Herrero[6], P. Esquej[7,8,9], C. Ramos Almeida[1,2], R. Mason[10], and C. Telesco[11]

[1] Instituto de Astrofísica de Canarias (IAC), C/Vía Láctea, s/n, E-38205 La Laguna, Spain
[2] Departamento de Astrofísica, Universidad de La Laguna, E-38205 La Laguna, Spain
[3] Juan de la Cierva Fellow (omairagm@iac.es)
[4] Spitzer Science Center, CalTech, Pasadena, CA 91125, USA
[5] Dept. of Physics & Astronomy, University of Texas San Antonio, Texas 78249, USA
[6] Augusto Gonzalez Linares Senior Research Fellow
[7] Instituto de Física de Cantabria, CSIC-Universidad de Cantabria, 39005 Santander, Spain
[8] Departamento de Física Moderna, Universidad de Cantabria, 39005 Santander, Spain
[9] Centro de Astrobiología, INTA-CSIC, E-28850 Madrid, Spain
[10] Gemini Observatory, 670 N. A'ohoku Place, Hilo, HI 96720, USA
[11] Department of Astronomy, University of Florida, Gainesville, Florida 32611, USA

Abstract

The unified model of active galactic nuclei (AGN) claims that the properties of AGN depend on the viewing angle of the observer with respect to a toroidal distribution of dust surrounding the nucleus. Both the mid-infrared (MIR) attenuation and continuum luminosity are therefore expected to be related to dust associated with the torus. We have compiled all the T-ReCS spectra (Gemini observatory) available in the N-band for 22 AGN: 5 Type-1 and 17 Type-2 AGN. We have used a novel pipeline called RedCan capable of producing flux- and wavelength-calibrated spectra for the CanariCam and T-ReCS instruments. We have also compiled *Spitzer*/IRS spectra for them. We have studied the star-formation and obscuration properties of our sample of AGN as seen in the MIR.

1 Introduction

The radiation from active galactic nuclei (AGN) is due to accretion onto a super-massive black hole (SMBH). The optical spectra of AGN have been classified into two main classes according to the existence (Type-1) or not (Type-2) of broad permitted lines (FWHM >2000 km s^{-1}). The *so-called* unified model proposes that both types of AGN are essentially the same objects viewed at different angles [1]. An optically-thick dusty torus surrounding the central source would be responsible for blocking the region where these broad emission lines are produced (the *so-called* broad line region, BLR). Therefore, Type-2 AGN would be essentially Type-

1 AGN blocked by the dusty torus along the line of sight (LOS) to the observer. More elaborated models suggest that the same observational constraints can also be explained with a torus made of discrete dense molecular clouds following a certain radial distribution [9, 5, 13, 14, 11]. MIR spectroscopy is a powerful tool to examine the nature of AGN, as well as the contribution of star-formation activity. The silicate features at 9.7μm and 18μm in Type-1 Seyfert galaxies are rather weak, while Type-2 Seyfert galaxies are likely to show strong silicate absorptions [21]. Furthermore, the deepest silicate absorption features show the highest values for the hydrogen column density (N_H) in X-rays [18].

We have compiles all the AGN observed by T-ReCS in the Gemini observatory. The sample comprises 22 AGN, including 9 Compton-thick sources (i.e. $N_H > 1.5 \times 10^{24}\,cm^{-2}$). Seventeen are Type-2 and five are Type-1 AGN. Taking into account the T-ReCS slit width, this results in a spatial resolution between $\sim 7 - 236$ pc for all the objects except for 3C 445 (406 pc), which is by far the most distant object in the sample. Our main aims are: (1) to characterize the AGN pure emission at MIR frequencies; (2) to understand the nature of the attenuation seen at MIR frequencies as traced by the optical depth at 9.7μm; (3) to compare T-ReCS and *Spitzer* spectra to understand the limitations introduced by the lower spatial resolution in *Spitzer* spectra.

2 Data reduction pipeline: RedCan

Data reduction pipelines are an important aspect of modern astronomy. Indeed large telescope instruments are becoming fairly complex, hence the prompt availability of science data is crucial for securing a fast scientific turnout from today's large and expensive facilities. Unfortunately, this is not always the case, even in successful facilities. The aim of our group is to produce a new and advanced pipeline for MIR imaging and spectroscopic data. In the forthcoming years large amounts of GTC/CanariCam data will be acquired by our group. This includes data from both guaranteed CanariCam time (∼100 hours, PI C. Telesco) and the ESO/GTC proposal led by A. Alonso-Herrero (∼180 hours, ESO/GTC 182.B.2005). It is therefore important to have a data reduction pipeline that facilitates the use of the data as soon as possible after being acquired at the telescope. This is the purpose of RedCan, the Canaricam data reduction pipeline we have developed. This pipeline is able to produce flux-calibrated images and 1D spectra for both the T-ReCS [19] and the CanariCam[1] [20] instruments without user interaction. This pipeline can be freely accessed[2] in order to facilitate a better exploitation of the CanariCam data.

3 The 11.3 μm PAH feature

The presence of polycyclic aromatic hydrocarbons (PAHs) has been associated to regions of star-formation, given the global correlations between star formation activity and PAH

[1]CanariCam is a mid-infrared (7.5 - 25μm) imager with spectroscopic, coronagraphic, and polarimetric capabilities, which is mounted at one of the Nasmyth foci of the GTC telescope at El Roque observatory.

[2]https://www.dropbox.com/sh/w4z8buo2ewrhhvj/Kk1f2RYVe8/RedCan.tar.gz

strength [16]. This emission is thought to originate in photo-dissociation regions (PDRs) where aromatic molecules are shielded from the radiation field produced by hot stars.

A strong PAH feature at 11.3 μm is present only in NGC 1808 and NGC 7130 in the T-ReCS spectra. A hint of this PAH feature is also present in other 3 AGN (NGC 1386, NGC 5643, and NGC 7172). Thus, for 15 out of 20 sources the high spatial resolution T-ReCS spectra are free of signs of star-formation at MIR wavelengths, as traced by the PAHs. When we compare the T-ReCS and the *Spitzer*/IRS spectra, in most cases the PAH emission comes from emitting regions outside of 7-130 pc (depending on distance) of the AGN. This is consistent with previous studies that suggested that AGN lack strong PAH features [6, 8, 10].

4 The [S IV] emission line at 10.5 μm

Another widely used AGN diagnostic line is the [SIV] at 10.5 μm since this line is thought to originate in the Narrow Line Region (NLR) [3]. However, the [SIV] at 10.5μm line arises from ions with ionization potential of 35 eV (similar to the optical line [O II] at 3727Å). Thus, this line can be produced in star-forming regions as well as in AGN [15].

The [SIV] line is detected in 11 AGN and a hint of this line is also present in two other sources with T-ReCS. In all cases it is also detected with *Spitzer*. Interestingly, *Spitzer* detected this line in other five sources (NGC 1365, NGC 1808, Circinus, 3C 445, and NGC 7479). One possibility is that the NLR has a preferential axis. This was already suggested in the case of IC 4518W [4]. Another possibility is that this line-emitting material is embedded in the dust, attenuating the emission of this line in the inner parts of the nuclei. Thus, the detection of this line as an AGN tracer should be taken with caution when the AGN have deep silicate features.

5 X-ray to MIR relation

The MIR emission in AGN originates from the reprocessing of the soft X-ray and UV radiation by the dust located in the torus. The reprocessed dust emission should then produce a significant correlation between X-ray luminosity (after corrected from X-ray absorption) and MIR luminosity. Fig. 1 (left) shows the absorption corrected 2-10 keV luminosity $L_{2-10\ \mathrm{keV}}$ versus the 12 μm luminosity $L_{12\,\mu\mathrm{m}}$. X-ray errors represent the expected X-ray variability among AGN of 0.5 dex while the MIR errors are inferred from the error on flux including 10% error for the total flux calibration. Most of the objects follow the same correlation found for AGN [12, 2]. Moreover, even those objects with significantly higher MIR emission compared to the X-rays are far from the correlation found for starburst galaxies (dot-dashed line in Fig. 1, right) [2]. Thus the AGN dominates the continuum emission at MIR frequencies.

6 The silicate absorption/emission feature

The silicate feature in Type-1 Seyferts is rather weak while in Type-2 Seyferts it is more likely to display strong silicate absorption using *Spitzer*/IRS data [21]. Only the spectra of NGC 1365 and 3C 445 show silicate features in emission and NGC 3081 shows very little absorption in the T-ReCS spectra.

The observed apparent optical depth at $\lambda \sim 9.7\,\mu$m can be measured as the ratio between the expected continuum flux ($f_{9.7,\rm cont}$) and the observed one ($f_{9.7,obs}$) [18]: $\tau_{9.7} = ln(f_{9.7,\rm cont}/f_{9.7,\rm obs})$. Sources with absorption (emission) features show positive (negative) optical depths. To estimate $f_{9.7,\rm cont}$ we have fitted the continuum to a linear relation to the 8.5 μm and 12.5 μm flux of each object. Fig. 1 (middle) shows $\tau_{9.7}$ versus $N_{\rm H}$ in logarithmic scale. For comparison purposes we have included the high angular resolution data for AGN observed with VISIR/VLT and Compton-thick AGN observed with *Spitzer*/IRS [10, 7].

We have tried to model this relationship under two assumptions: (1) the uniform dusty torus model and (2) the clumpy torus models. The uniform dusty torus is not able to explain large $N_{\rm H}$. Clumpy torus models are able to explain why highly obscured objects at X-rays show low optical depths at 9.7μm. However, the model fails to reproduce more than a dozen of sources with high value for ($\tau_{9.7} > 1$, see Fig. 1, middle). We find that all the objects with high $\tau_{9.7}$ are hosted in galaxies with high inclination angles and/or mergers, and/or nuclear dust lanes (see Fig. 1, left). We find that, in general, the clumpy torus model can only explain face-on galaxies free of either dust lanes and/or participating in mergers. Only three objects show one of these properties without a strong ($\tau_{9.7} < 0.4$) silicate absorption feature that can be reproduced by clumpy models (IC 4329A, NGC 3227, and NGC 424). Therefore, *we conclude that even at the high angular resolutions (100 pc) of our observations, dust in the host galaxy can play a role on the overall dust extinction seen at MIR frequencies, and particularly it does when deep silicate absorption features are measured.*

7 Conclusions

Here we present an analysis of 20 high spatial resolution MIR AGN spectra observed with T-ReCS (Gemini observatory) at scales of ∼100 pc. T-ReCS data have been processed with the pipeline RedCan. RedCan has been developed by our group for the data reduction for the imaging and spectroscopic modes of the CanariCam instrument, recently available at the GTC (La Palma, Spain).

The 11.3 μm PAH feature is only clearly detected in the nuclear spectra of two AGN, while it is more common among *Spitzer* data. For these two objects the AGN emission accounts for more than 80% of the MIR continuum at 12 μm. This is confirmed by the correlation between the MIR and X-ray continuum luminosities. The [S IV] emission line at 10.5μm, which is believed to originate in the narrow line region, is detected in most of the AGN studied here. Interestingly, in some objects it is detected in the *Spitzer* spectrum but not in the nuclear T-ReCS one. We suggest that this line is affected by dust attenuation at the inner regions of the AGN. This is consistent with the non-detection of this line for the objects

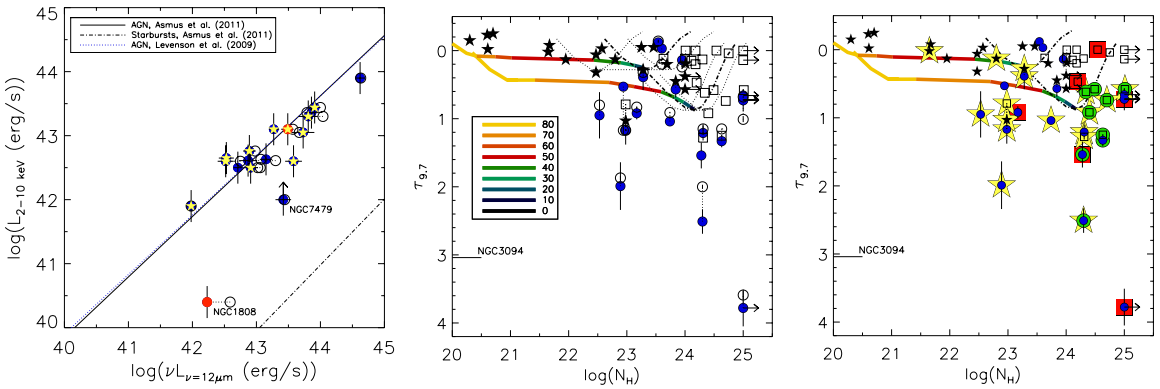

Figure 1: *Left panel:* Absorption corrected 2-10 keV luminosity versus the 12 μm luminosity. Filled circles are T-ReCS data and open circles are *Spitzer* data. Yellow stars and red circles mark the objects with the strongest [SIV]10.5 μm and PAH at 11.3 μm emissions in the T-ReCS spectra, respectively. The blue dotted line shows the best fit for AGN [12]. Black dotted-dashed and solid lines represent the best fit for Starburst galaxies and AGN, respectively [2]. *Center panel:* The optical depth at 9.7μm, $\tau_{9.7}$ versus the logarithmic of the hydrogen column density at X-rays, N_H. N_H in units of cm^{-2}. [7]: Compton-thick sources are shown as open squares. [10]: AGN observed with VISIR/VLT are shown as black-filled stars. The curves are are the CLUMPY model predictions for $i = 0°$ and $N_o = [5, 25]$ clouds. *Right panel:* Edge-on galaxies are shown as big red squares, galaxies with dust-lanes are shown with big yellow stars, and mergers are shown as big green circles. Note that edge-on galaxies are shown only when dust-lanes are not present for clarity of the plot.

showing the deepest silicate feature. We have found an enhancement of the optical depth at 9.7μm in the high-angular resolution data for higher values of N_H. Clumpy torus models reproduce the observed values *only* if the host-galaxy properties are taken into account.

Acknowledgments

The authors acknowledge the Spanish MINECO through project Consolider-Ingenio 2010 Program grant CSD2006-00070: First Science with the GTC (http://www.iac.es/consolider-ingenio-gtc/). This work was also partially funded by the Spanish MINECO through a Juan de la Cierva Fellowship.

References

[1] Antonucci, R. 1993, ARAA, 31, 473

[2] Asmus, D., Gandhi, P., et al. 2011, A&A, 536, A36

[3] Dasyra, K. M., Ho, L. C., Netzer, H., et al. 2011, ApJ, 740, 94

[4] Díaz-Santos, T., Alonso-Herrero, A., Colina, L., et al. 2010, ApJ, 711, 328

[5] Elitzur, M. 2008, Nature, 52, 274

[6] Genzel, R., Lutz, D., Sturm, E., et al. 1998, ApJ, 498, 579

[7] Goulding, A. D., Alexander, D. M., Bauer, F. E., et al. 2012, arXiv:1205.1800

[8] Hernán-Caballero, A., et al. 2009, MNRAS, 395, 1695

[9] Hönig, S. F., Beckert, T., Ohnaka, K., & Weigelt, G. 2006, A&A, 452, 459

[10] Hönig, S. F., Kishimoto, M., Gandhi, P., et al. 2010, A&A, 515, A23

[11] Hönig, S. F. & Kishimoto, M. 2010, A&A, 523, A27

[12] Levenson, N. A., Radomski, J. T., Packham, C., et al. 2009, ApJ, 703, 390

[13] Nenkova, M., Sirocky, M. M., Ivezić, Ž., & Elitzur, M. 2008, ApJ, 685, 147

[14] Nenkova, M., Sirocky, M. M., Nikutta, R., et al. 2008, ApJ, 685, 160

[15] Pereira-Santaella, M., et al. 2010, ApJS, 188, 447

[16] Roche, P. F., et al. 1991, MNRAS, 248, 606

[17] Roche, P. F., Packham, C., Telesco, C. M., et al. 2006, MNRAS, 367, 1689

[18] Shi, Y., Rieke, G. H., Hines, D. C., et al. 2006, ApJ, 653, 127

[19] Telesco, C. M., Pina, R. K., et al. 1998, Proc. SPIE, 3354, 534

[20] Telesco, C. M., Ciardi, D., et al. 2003, Proc. SPIE, 4841, 913

[21] Wu, Y., Charmandaris, V., Huang, J., Spinoglio, L., et al. 2009, ApJ, 701, 658